

NDON/CR 1998- 207058

FINAL  
NCC3-493  
0017  
005533



**STRUCTURAL SYSTEMS  
RESEARCH PROJECT**

Report No.  
SSRP - 98/01

**EXPERIMENTAL SPIN TESTING OF  
INTEGRALLY DAMPED COMPOSITE  
PLATES**

by

**John Kosmatka**

Final Report on a Research Project funded through NASA  
Research Grant Number NCC3-493.

February 1998

Division of Structural Engineering  
University of California, San Diego  
La Jolla, California 92093-0085



Structural Systems Research Project

Report No. SSRP-98/01

**EXPERIMENTAL SPIN TESTING OF INTEGRALLY  
DAMPED COMPOSITE PLATES**

by

**John Kosmatka**

Final Report on a Research Project funded through  
NASA Research Grant Number NCC3-493.

February 1998



## Table of Contents

	<b><u>Page</u></b>
ABSTRACT	1
1. INTRODUCTION	2
2. PLATE DEFINITION	3
3. NASA-LEWIS SPIN FACILITY / TEST PLAN	5
4. TEST RESULTS	7
5. CONCLUSIONS	25
6. REFERENCES	26

## Table of Figures

	<u>Page</u>
Fig. 1 Set One, Flat Plate Configurations	4
Fig. 2 Set Two, Pretwisted Plate Configurations	4
Fig. 3.a: NASA-Lewis Spin Facility	6
Fig. 3.b: Clamp and Trunnion Assembly	8
Fig. 4.a NASA-Lewis Laser Holography Results for a <u>Baseline Flat</u> Plate	9
Fig. 4.b NASA-Lewis Laser Holography Results for a <u>First Mode Damping Flat</u> Plate	10
Fig. 4.c NASA-Lewis Laser Holography Results for a <u>All Mode Damped Flat</u> Plate	11
Fig. 4.d NASA-Lewis Laser Holography Results for a <u>Baseline Pretwisted</u> Plate	13
Fig. 4.e NASA-Lewis Laser Holography Results for <u>First Mode Damp Pretwisted</u> Plate	14
Fig. 4.f NASA-Lewis Laser Holography Results for a <u>All Mode Pretwisted</u> Plate	15
Fig. 5.a Experimentally Measured Frequency Response Functions: First Chord-wise Mode of Undamped and Damped Plates ( $\Omega = 0$ rpm)	16
Fig. 5.b: First and Second Bending Mode Frequency Response Functions for Flat Plates	17
Fig 6.a: Variation of 1st Bending Frequency with Rotor Speed Flat Plate	18

## Table of Figures (continued)

	<b><u>Page</u></b>
Fig 6.b: Variation of 1st Bending Damping with Rotor Speed Flat Plate	18
Fig 7.a: Variation of 2nd Bending Frequency with Rotor Speed Flat Plate	19
Fig 7.b: Variation of 2nd Bending Damping with Rotor Speed Flat Plate	19
Fig 8.a: Variation of 1st Torsion Frequency with Rotor Speed Flat Plate	20
Fig 8.b: Variation of 1st Torsion Damping with Rotor Speed Flat Plate	20
Fig 9.a: Variation of 1st Bending Frequency with Rotor Speed for Twisted Plates	22
Fig 9.b: Variation of 1st Bending Damping with Rotor Speed for Twisted Plates	22
Fig 10.a: Variation of 2nd Bending Frequency with Rotor Speed for Twisted Plates	23
Fig 10.b: Variation of 2nd Bending Damping with Rotor Speed for Twisted Plates	23
Fig 11.a: Variation of 2nd Bending Frequency with Rotor Speed for Twisted Plates	24
Fig 11.b: Variation of 2nd Bending Damping with Rotor Speed for Twisted Plates	24

# Experimental Spin Testing of Integrally Damped Composite Plates

## ABSTRACT

The experimental behavior of spinning laminated composite pretwisted plates (turbo-fan blade-like) with small (less than 10% by volume) integral viscoelastic damping patches was investigated at NASA-Lewis Research Center. Ten different plate sets were experimentally spin tested and the resulting data was analyzed. The first four plate sets investigated tailoring patch locations and definitions to damp specific modes on spinning flat graphite/epoxy plates as a function of rotational speed. The remaining six plate sets investigated damping patch size and location on specific modes of pretwisted (30 degrees) graphite/epoxy plates. The results reveal that: (1) significant amount of damping can be added using a small amount of damping material, (2) the damped plates experienced no failures up to the tested 28,000 g's and 750,000 cycles, (3) centrifugal loads caused an increase in bending frequencies and corresponding reductions in bending damping levels that are proportional to the bending stiffness increase, and (4) the centrifugal loads caused a decrease in torsion natural frequency and increase in damping levels of pretwisted composite plates.

## 1. INTRODUCTION

Reducing fan blade vibrations is of prime importance to increasing gas turbine engine blade reliability and durability. It is well known that vibration reductions can be achieved by adding damping to metal and composite blade-disk systems. A series of experiments were performed to investigate the use of integral viscoelastic damping treatments to reduce vibrations of rotating composite fan blades. This is part of a joint research effort with NASA Lewis Research Center and the University of California, San Diego (UCSD). Previous vibration bench (nonspinning) tests obtained at UCSD (reference [1]) show that plates with embedded viscoelastic materials had over ten times the damping as similar undamped composite plates. Moreover, these increases in damping were found without a noticeable decrease in blade stiffness. The objectives of this series of experiments were to verify the structural integrity of composite plates with viscoelastic damping materials embedded between composite layers while under large steady in-plane spin-produced centrifugal forces, and to measure the damping and natural frequencies as a function of rotational speed.

While no previous analytical or experimental studies have investigated the effects of integral damping treatments on the behavior of composite turbo-fan blades (i.e. pretwisted composite damped structures subjected to large in-plane centrifugal loads), the following relevant studies provide insight into the current design and analysis procedures. In [2], the vibrational and damping characteristics of undamped composite pre-twisted plates have been studied, where the effects of pre-twist angle, ply lay-up, taper, and skew on the frequency and damping have been addressed. A simple design and analysis procedure [3] has been developed for simply supported semi-infinite integrally-damped composite plates having carbon composite face sheets sandwiching 3M Scotchdamp ISD-112. This approach first determines the maximum damping for a given damping layer thickness and then the ply orientation is varied to study changes in the overall plate stiffness and damping. Analytical results were presented in [4] showing that particular vibration modes can be selectively damped by varying the patch size and location of the attached constraining damping material for cantilevered composite (glass-epoxy) beams. Saravanos and Pereira [5] investigate the damping of simply supported composite plates looking at effects such as aspect ratio, damping layer thick-

ness and fiber volume ratio on the modal characteristics. In [6], the placement (size, location) of integral treatments in flat and pretwisted composite plates are studied by both analytical and experimental techniques.

## 2. PLATE DEFINITION

Two different sets of plates were fabricated for initial bench testing (mode shapes, frequencies, damping levels) and then a down-selection process was performed to minimize the number of plates for spin testing. The first plate set involved four different laminated composite flat plate (9" x 3" x 0.045") pairs. The plates are sandwich-like in that they have upper and lower face sheets and a central damping layer. See Figure 1. The face sheets are a composite laminate defined using pre-impregnated unidirectional T-300/934 HYE 1034C carbon fiber tape. The central layer damping material is 3M Scotchdamp ISD 113 viscoelastic polymer (ISD-113) and the material for the remaining central layer was either; (1) T-300/934 HYE 1034C carbon fiber tape in a (0°) orientation, (2) T-300/934 HYE 1034C carbon fiber tape in a (90°) orientation, or (3) 3M Scotch-Weld AF-32 structural adhesive film (AF32). The four plate pairs involved two different baseline plates, a plate pair to damp all modes and a pair to damp specifically the first bending mode. The configuration to damp the first mode involved putting a small 2" by 2" layer near the cantilever root, whereas the laminate to damp all modes had a 2" by 8" patch with a 0.5" border of AF-32 (structural adhesive). A loose-weave (0.100" open cell) nylon scrim cloth is also embedded in the damping material to keep the damping material from creeping outward under the large steady state (centrifugal) forces. Two baseline plates were also constructed; one with a graphite/epoxy central layer and one with a structural adhesive central layer. The entire laminate was symmetric to eliminate any problems of warping during cure, but the use of ( $\pm 15$  degrees) introduced minor bend-twist coupling effects which was observed in the mode shapes (NASA-Lewis Laser Holography). Also the plates had over 50% zero-degree fibers to provide sufficient axial and bending stiffness. Thus the fabricated laminates zero degree fibers on either side of the damping layer.

The second plate set (see Fig. 2), involved six pairs of damped composite plates having the same outer geometry (3" x 9" x 0.045") as the first set, except of the addition of a 30 degree

Fig. 1: Set One, Flat Plate Configurations

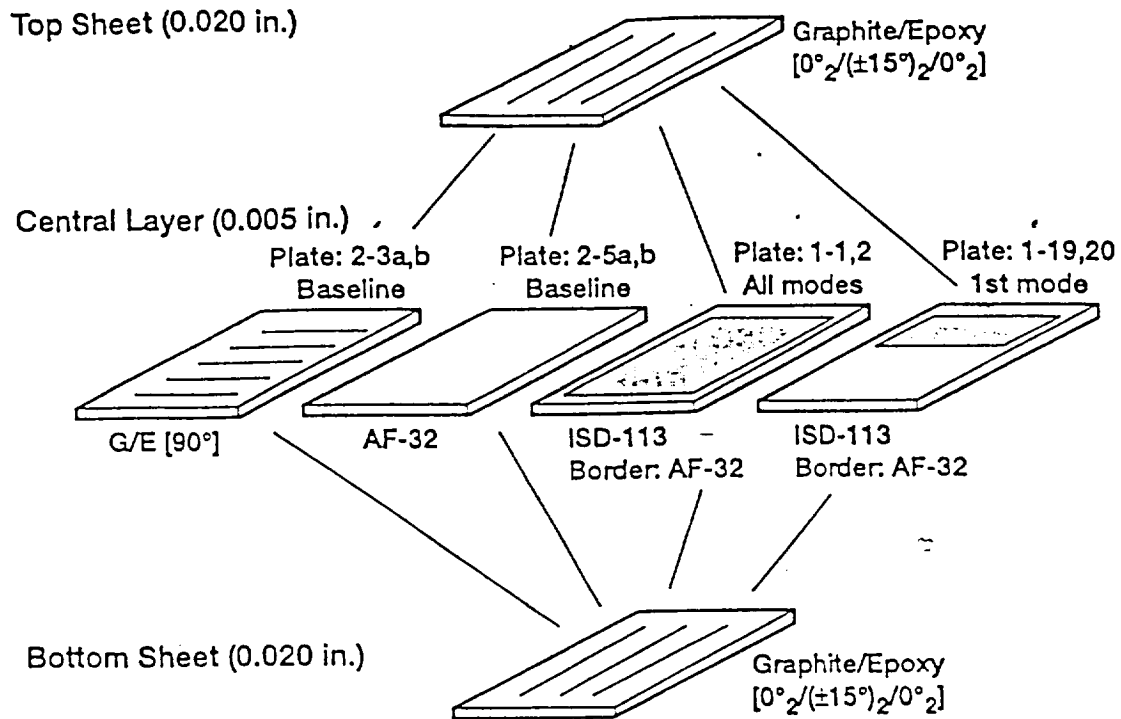
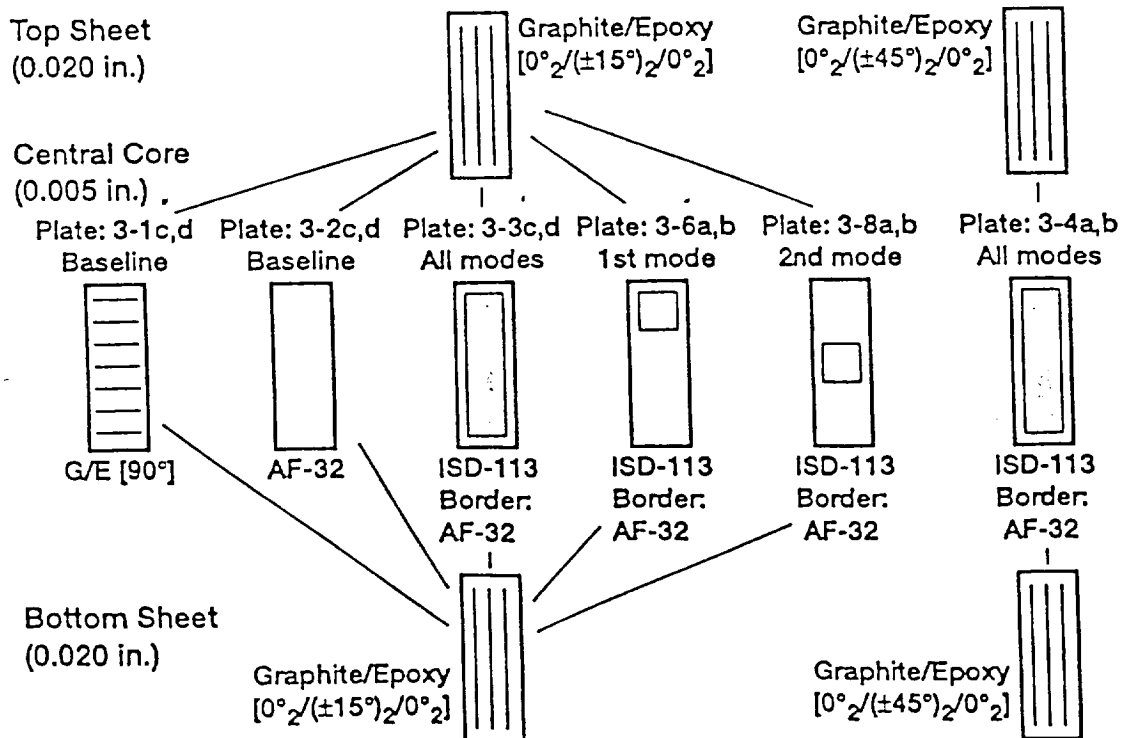


Fig. 2: Set Two, Pretwisted Plate Configurations

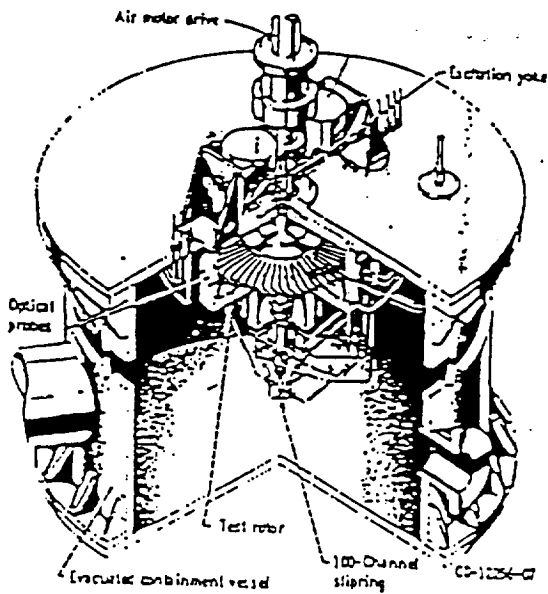


linear twist about the plate centerline. These plates were laid-up on a precise tool to control twist. Five plate pairs had the same upper/lower face sheets  $[0_2/(\pm 15)_2/0_2]$  but differing central layers: undamped (G/E 90° or AF-32), damped all modes (2" x 8" patch of ISD-113), damped first mode (2" x 2" patch of ISD-113 near root), and damped second mode (2" x 2" patch of ISD-113 near mid-length). A sixth plate pair was fabricated having slight different face sheet definitions  $[0_2/(\pm 45)_2/0_2]$ , but designed to damp all of the vibratory modes (2" x 8" patch of ISD-113).

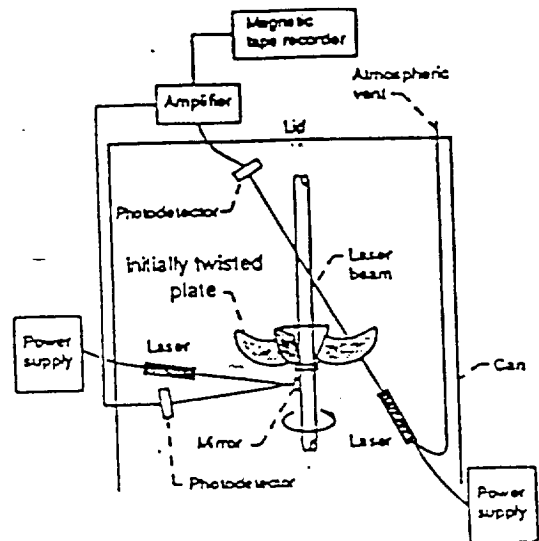
The central layer border of (0°) carbon fiber tape will provide the greatest structural integrity for the in-plane centrifugal loads, but it will also prevent a large amount of potential shear strain energy from entering the damping material patch, whereas a central layer composed of softer material (either 90° carbon tape or AF32 structural adhesive) will enable a much larger portion of shear strain energy to enter the damping material patch. Thus greatly increasing the overall modal damping levels. An all VEM central ply was not considered for our studies because the VEM has such low structural properties that may creep or delaminate as a result of the large expected centrifugal loads.

### **3. NASA-LEWIS SPIN FACILITY / TEST PLAN**

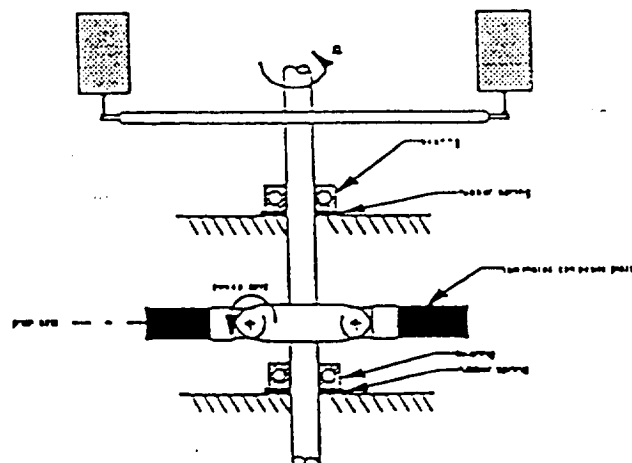
The experiment was performed in the NASA-Lewis Dynamic Spin Facility, a drawing of the installation is shown in Figure (3.a). This is a spin rig facility where the shaft can be vibrated while stationary or spinning to cause blade vibration by base motion. The shaft is air turbine driven, has a vertical axis of rotation, and is supported at the top end by a ball bearing on compliant mounts to allow small shaft motions. There is a magnetic bearing at the lower shaft end. The lower magnetic bearing is used to both support the shaft and to force shaft vibration. Proximeter probes are used to sense shaft motion for control of the magnetic bearing. A random noise signal centered in bandwidth about the plate modes of interest was used for the excitation to the magnetic bearing. Above rotational speeds of 4000 rpm, there were significant signal-to-noise problems which made it difficult to get accurate results. The best way to overcome this was to increase the amplitude of the bearing excitation and increase the



NASA-Lewis Dynamic Spin Rig Facility



Laser deflection measurement system



Spinning plate setup at the NASA Lewis Research Center

Fig. 3.a: NASA-Lewis Spin Facility

number of ensemble averages (typically over 100 averages per dwell speed). The slip ring brushes and line electrical interference are believed to be the major source of the noise.

Two strain-gauged composite plate test specimens are attached to the hub structure through the use of quick-change clamps. See Figure (3.b) for clamp design. These clamps have: (1) a serrated clamp surface and sufficient shear area to grip the plate and insure that it can not be pulled out as a result of large centrifugal forces (8000 rpm produces 28,000 g's), (2) a 14-pin plug connector for quick-change, and (3) two embedded accelerometers to sense clamp base transverse vibrations and twist rotations. The radius of the blade tips is 396.2 mm (15.6 inch). The strain gages were located on the plates to provide a good signal amplitude of the particular modes (1st and 2nd bending and 1st torsion). The four strain gages on each plate were connected into a full Wheatstone bridge configuration to further increase the signal-to-noise ratio. Signals from bridges with only active blade gauge were not as high in amplitude, and in general, were closer to the noise floor.

Plate damping data was collected at dwells of rotation speed up to 8000 rpm (28,000 g's). Data was collected at 0 rpm, 500 rpm, 1000 rpm, 2000 rpm, 3000 rpm, 4000 rpm, 6000 rpm, and 8000 rpm. The total test time was estimated to accumulate 750,000 cycles on each blade set.

#### 4. TEST RESULTS

Initially, the modal properties (natural frequencies and mode shapes) of all ten "nonspinning" plate pairs were measured at NASA-Lewis Research Center in their Laser Holography Test Facility. Six examples are presented in Figures (4.a-f). These results were pretty much beam-like in that the lowest modes of the plate behaved like a cantilevered beam (first bend, second bend, first torsion, and third bend). The upper modes are more plate-like with more cross-section deformation (first chord-wise, second torsion, second chord-wise, and third torsion). In Figures (4.a-c), the holograms of the mode shapes are presented for three flat plates (baseline, damping first mode, damping all modes). Looking at these results it is clear that the damping patch doesn't significantly alter the shape of the global mode nor does it intro-

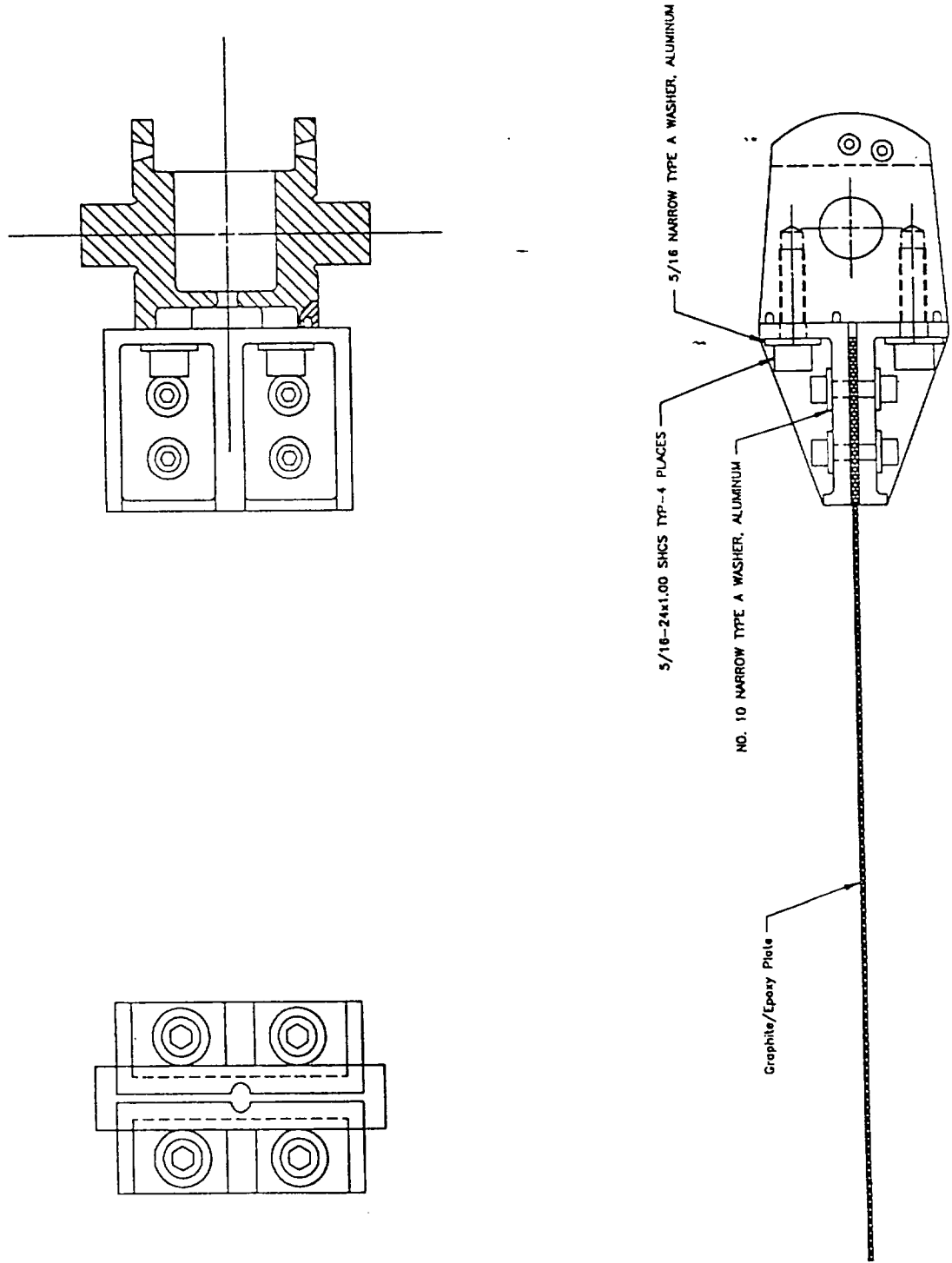
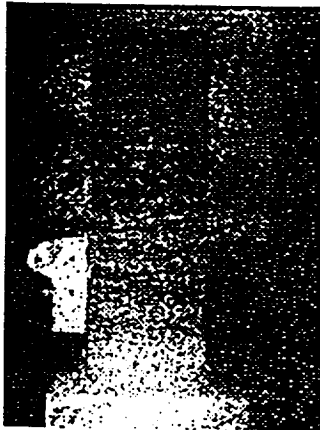


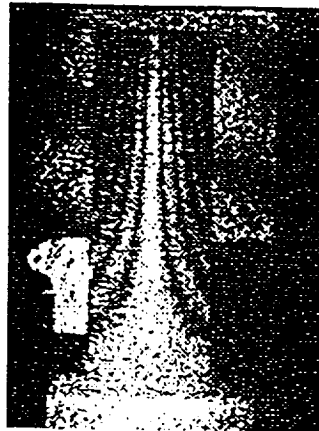
Fig. 3.b: CLAMP AND TRUNNION ASSEMBLY

# NASA-Lewis Laser Holography Results Plate 2-3a (Baseline)

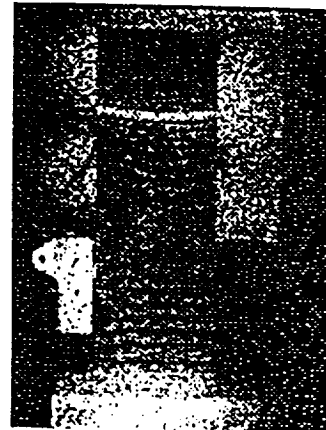
$[0_2/(\pm 15)_2/0_2/90]_S$



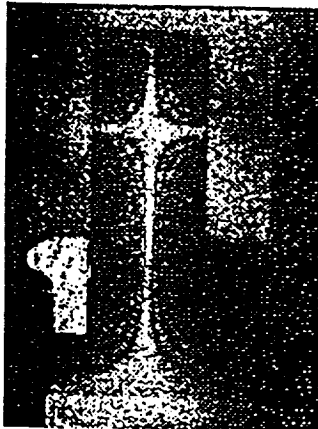
34 Hz. 2.2 V.



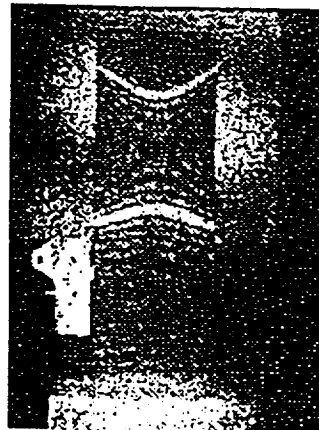
106 Hz. 0.4 V.



203 Hz. 0.04 V.



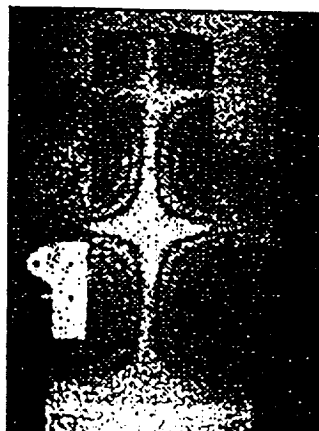
355 Hz. 0.1 V.



560 Hz. 0.01 V.



651 Hz. 0.9 V.

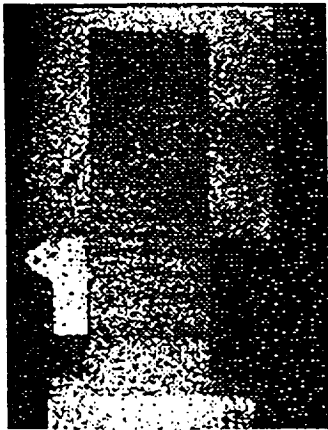


726 Hz. 0.4 V.

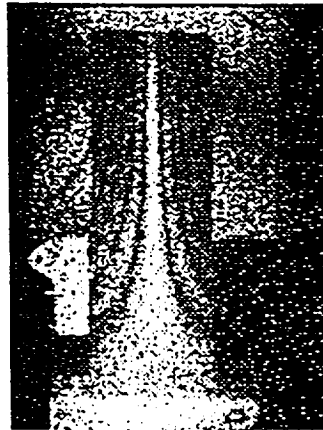
Fig. 4.a : NASA-Lewis Laser Holography Results for a Baseline Flat Plate

# NASA-Lewis Laser Holography Results Plate 1-19 (Damping 1st Mode)

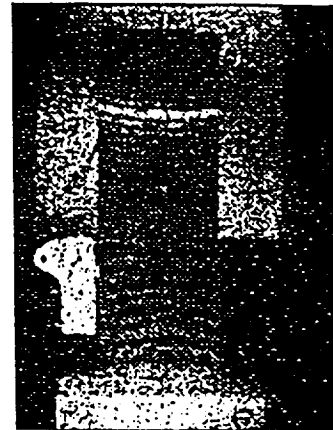
$[0_2/(\pm 15)_2/0_2/ISD-113]_S$



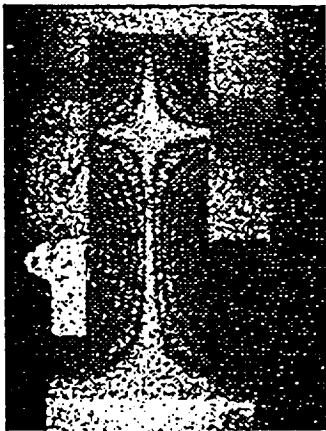
30 Hz. 4.0 V.



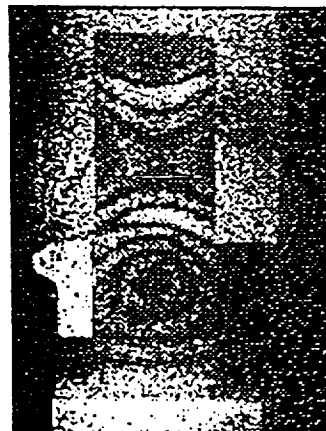
99 Hz. 0.9 V.



185 Hz. 0.5 V.



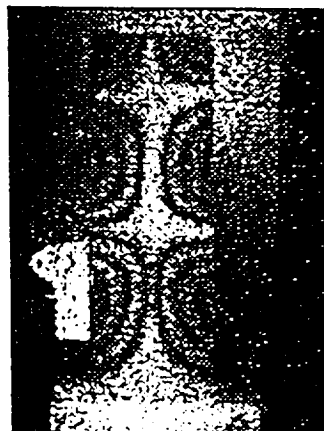
327 Hz. 0.3 V.



483 Hz. 0.6 V.



584 Hz. 1.0 V.

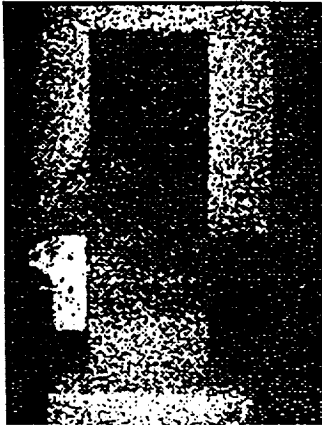


658 Hz. 1.0 V.

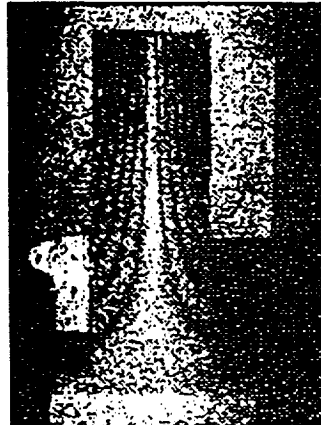
Fig. 4.b : NASA-Lewis Laser Holography Results for a First Mode Damped Flat Plate

# NASA-Lewis Laser Holography Results Plate 1-1 (Damping All Modes)

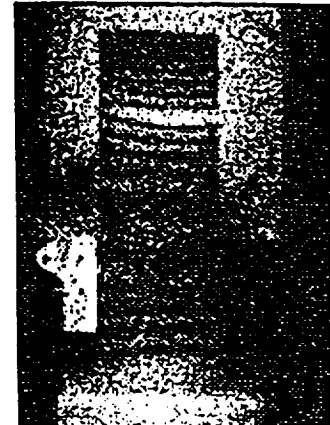
$[0_2/(\pm 15)_2/0_2/\text{ISD}-113]_S$



29 Hz. 4.7 V.



95 Hz. 1.2 V.



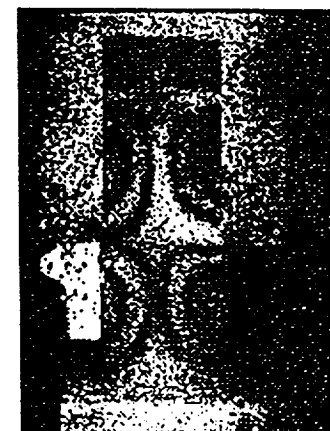
170 Hz. 1.0 V.



311 Hz. 0.2 V.



427 Hz. 1.1 V.



602 Hz. 1.0 V.

Fig. 4.c : NASA-Lewis Laser Holography Results for an All Mode Damped Flat Plate

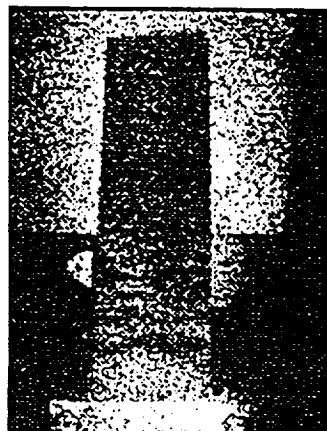
duce any local skin-panel modes. These modes look 'very isotropic' with minimal composite (bend-twist) coupling. In Figures (4.d-f), the holograms of the mode shapes are presented for three pretwisted plates (baseline, damping first mode, damping all modes). Again, from these figures it is clear that the damping patch doesn't alter the mode, doesn't introduce any local skin-panel modes, and there is minimal composite (bend-twist) coupling.

The plate natural frequencies and damping levels in the spin rig have been obtained from the measured transfer function of the plate strain gauge to clamp accelerometer signals. Transfer function data for the first chord-wise mode of the two baseline flat plates and a damped flat plate (1-19a) at zero rpm are shown in Fig. 5.a. The damping level of plate 1-19a, with the second mode patch design, is over two times that of the baseline plates; and the damping would be greater if the patch had been optimized for the chord-wise mode. This is the only chord-wise mode data obtained from the experiment because the strain gauges were not located to be sensitive to this mode. However, chord-wise modes are causing fatigue problems in modern engines and need to be damped. Future tests will concentrate on this mode.

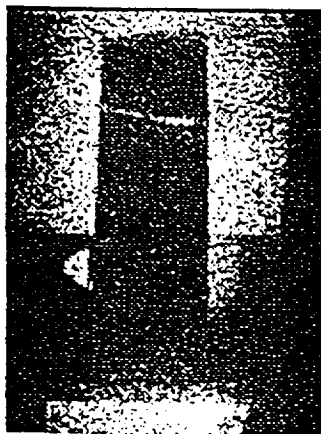
The signal to noise ratio was a problem at rotor speeds above 4000 rpm due to slip ring noise. A comparison of bending mode transfer functions of two different flat plate pairs at (0 rpm) and (4000 rpm) is presented in Figure 5.b. In both cases the base electrical noise (harmonics of 60 Hz) can be seen, but at by (4000 rpm) there is quite a bit of broad band noise. In these results it can be clearly seen the change in frequency and damping levels of the different plates with speed. Forty averages of each data record was taken to reduce the noise, but because of remaining noise, curve-fitting of the transfer function data was required before calculating damping values. On the noisiest plates over 100 averages were taken.

The compiled frequency and damping (loss factor) results of the spinning flat plate study is presented in Figure 6-8, for the first bending, second bending, and first torsion modes respectively. In Figures (6.a) and (6.b), the natural frequency and damping levels of the first bending mode of the four flat plates are presented as a function of rotational speed. Results could be determined up to 4000 rpm, where above that speed the frequency could be observed but the data was too noisy to determine the damping levels. These results clearly show the significant increase in bending frequency with rotor speed for all plates, as well as

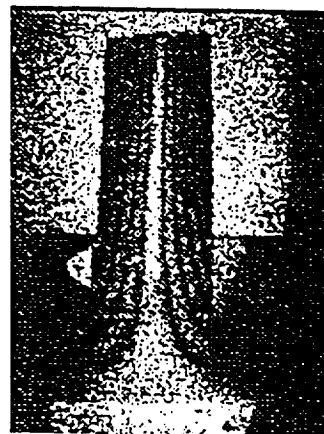
NASA-Lewis Laser Holography Results  
 Plate 3-1c (Baseline)  
 $[0_2/(\pm 15)_2/0_2/90]_S$



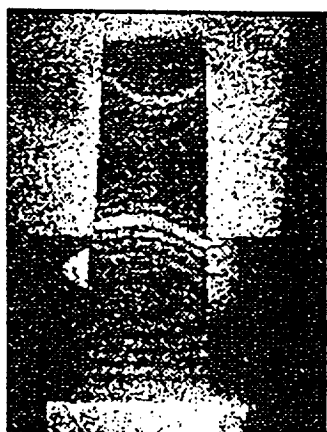
36 Hz. 3.0 V.



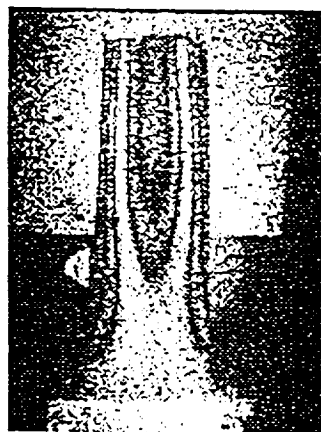
199 Hz. 0.04 V.



365 Hz. 0.04 V.



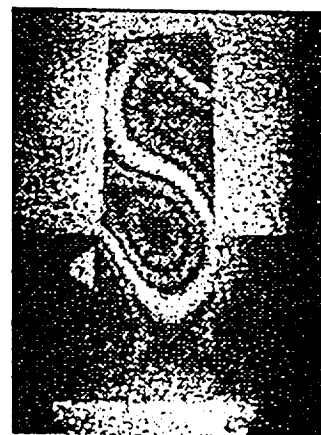
585 Hz. 0.04 V.



725 Hz. 0.8 V.



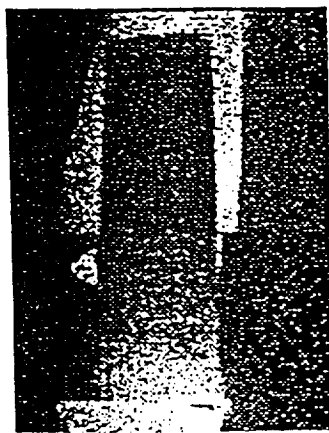
885 Hz. 0.5 V.



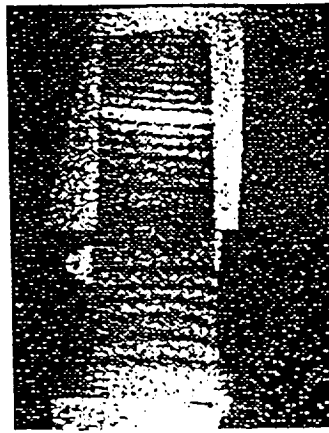
1172 Hz. 0.04 V.

Fig. 4.d : NASA-Lewis Laser Holography Results for a Baseline Pretwisted Plate

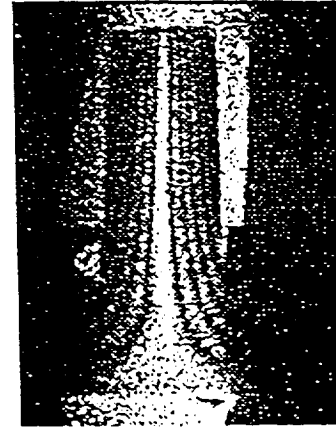
NASA-Lewis Laser Holography Results  
 Plate 3-6a (Damping 1st Mode)  
 $[0.2/(\pm 15) 2/0_2/ISD-113]_s$



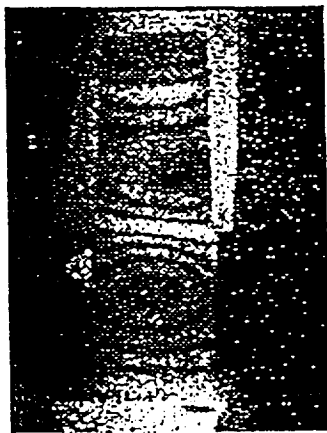
33 Hz. 4.0 V.



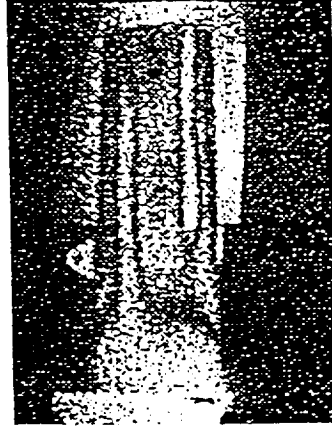
177 Hz. 0.4 V.



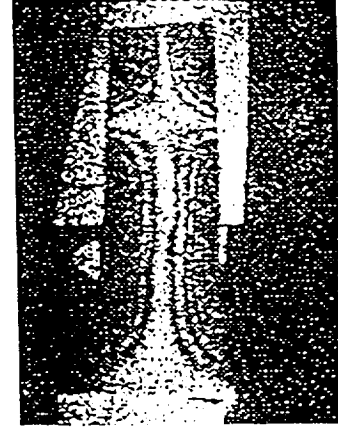
354 Hz. 0.1 V.



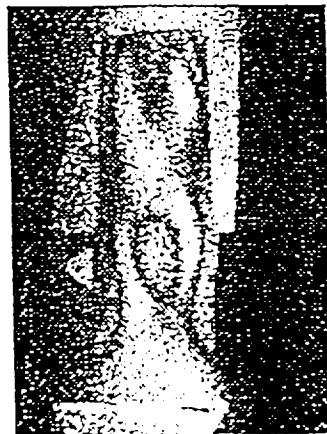
470 Hz. 0.5 V.



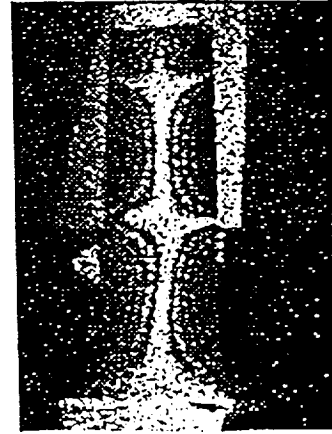
648 Hz. 1.5 V.



803 Hz. 1.0 V.



1002 Hz. 0.9 V.



1120 Hz. 0.3 V.

Fig. 4.e : NASA-Lewis Laser Holography Results for a First Mode Damped Pretwisted Plate

NASA-Lewis Laser Holography Results  
 Plate 3-3c (Damping All Modes)  
 $[0_2/(\pm 15)_2/0_2/ISD-113]_s$

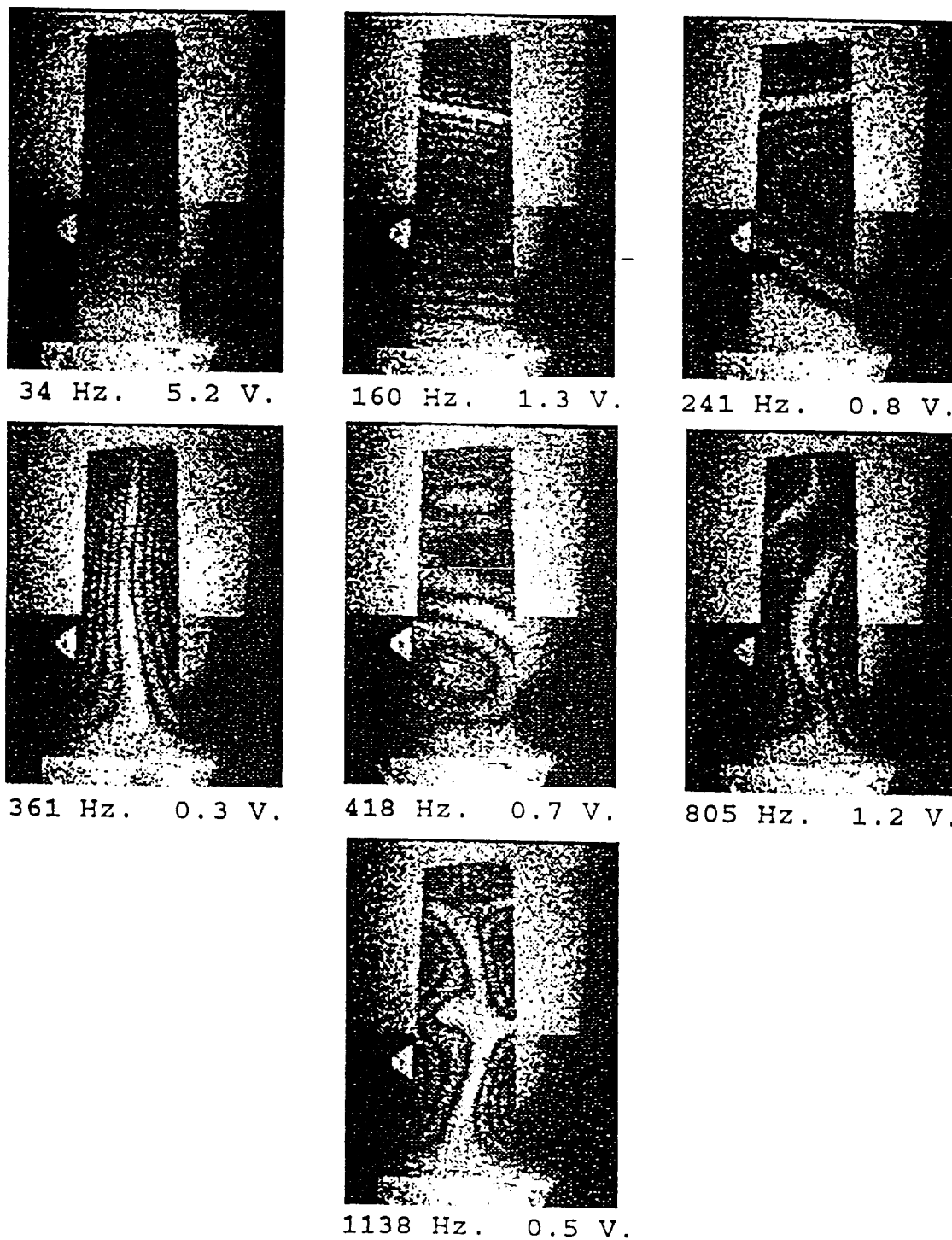


Fig. 4.f: NASA-Lewis Laser Holography Results for an All Mode Damped Pretwisted Plate

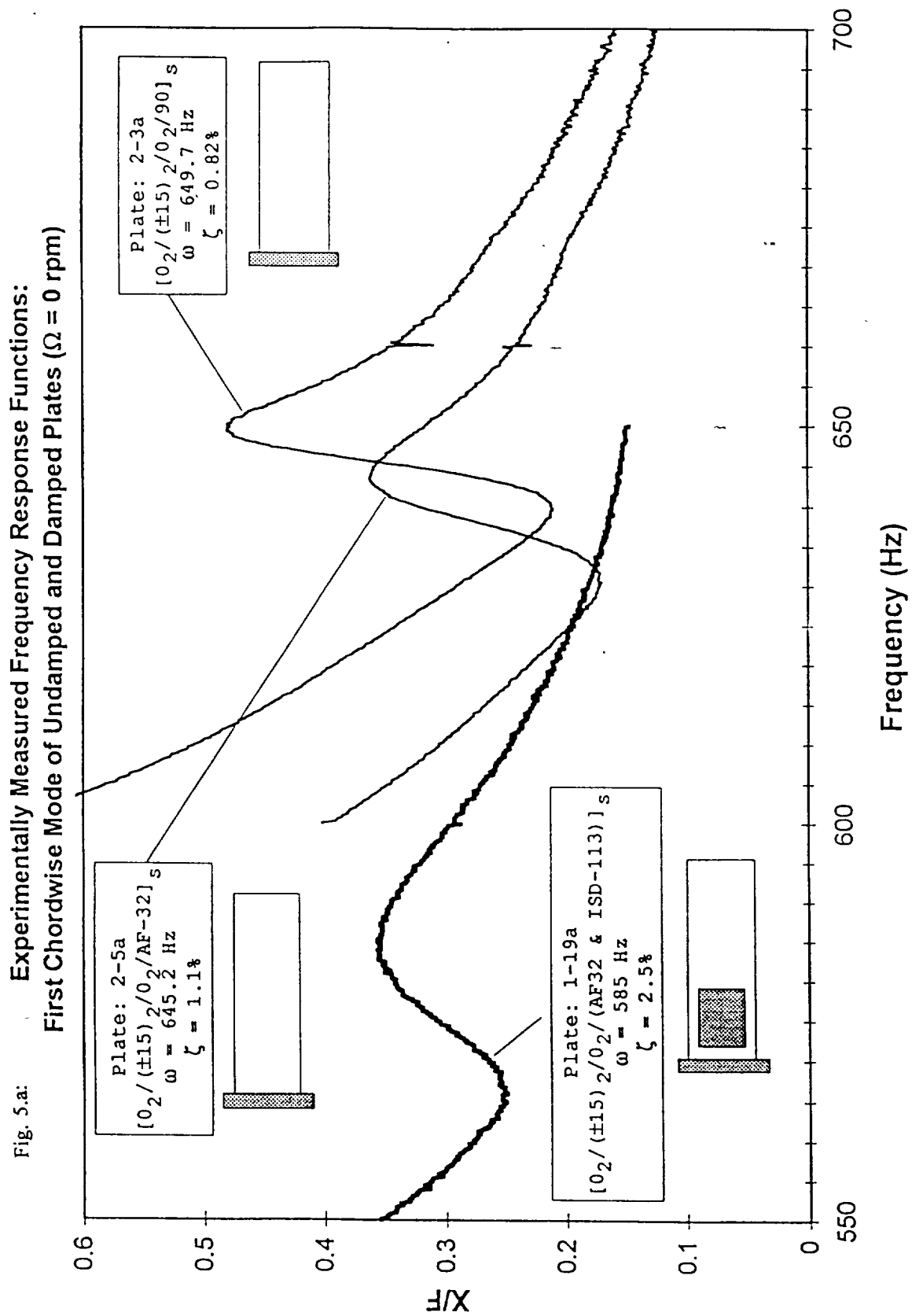
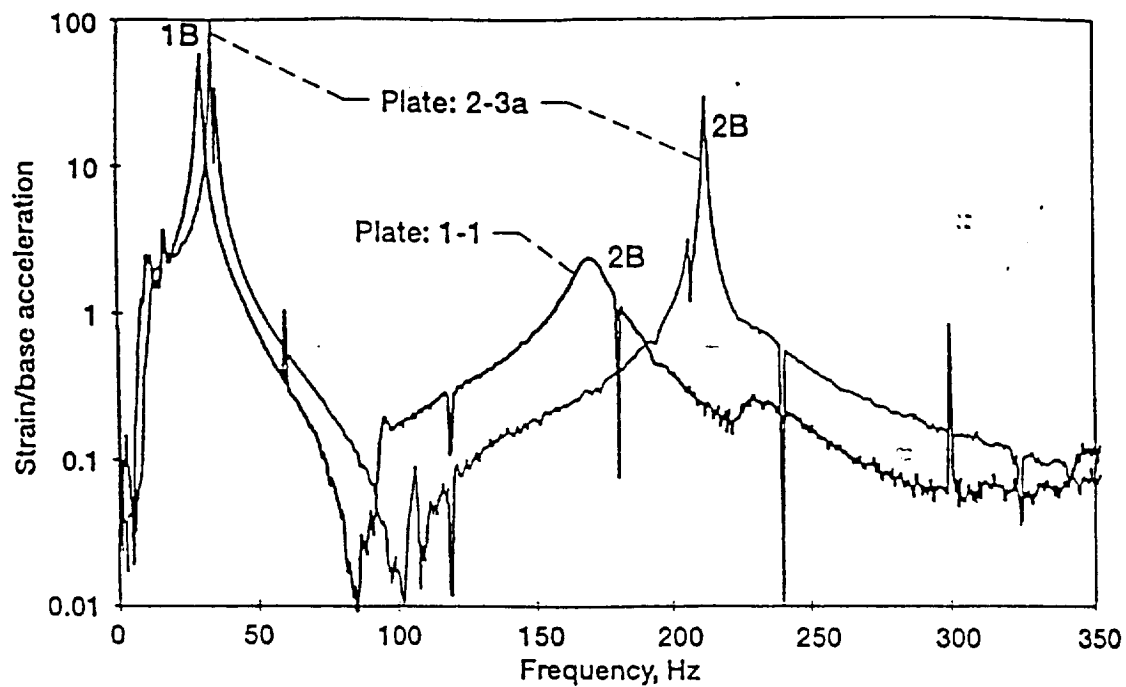


Fig. 5.b: First and Second Bending Mode Frequency Response Functions for Flat Plates

$\Omega = 0$  rpm



$\Omega = 4000$  rpm

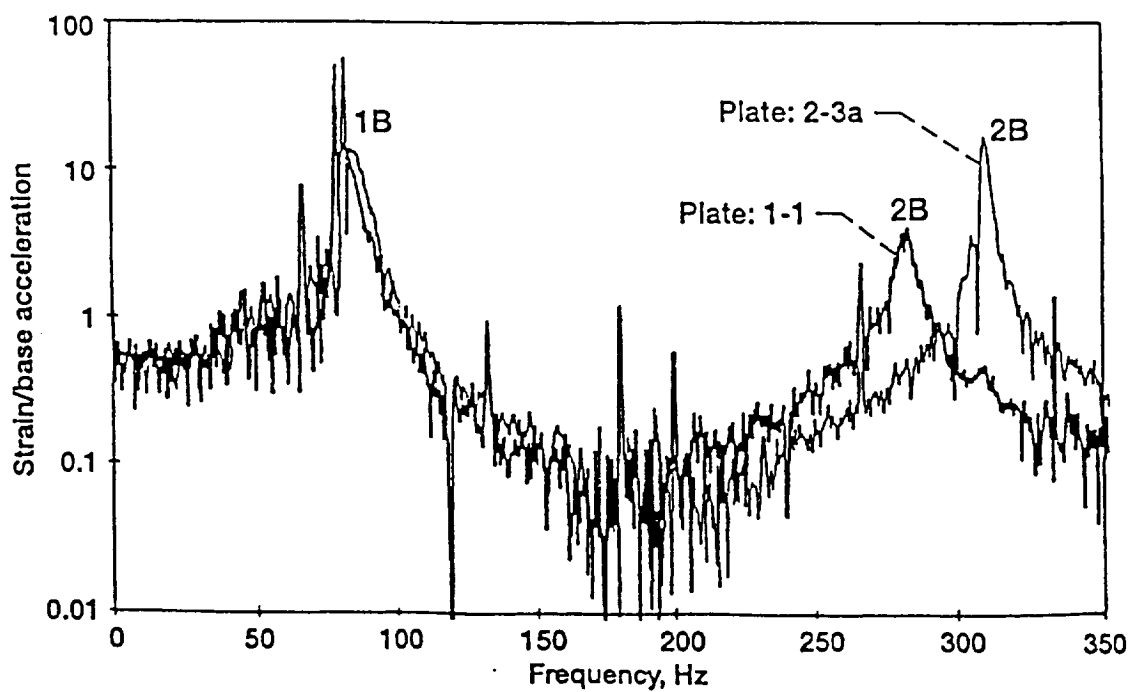


Fig. 6.a: Variation of 1st Bending Frequency (1st Peak) with Rotor Speed:  
Flat Plate

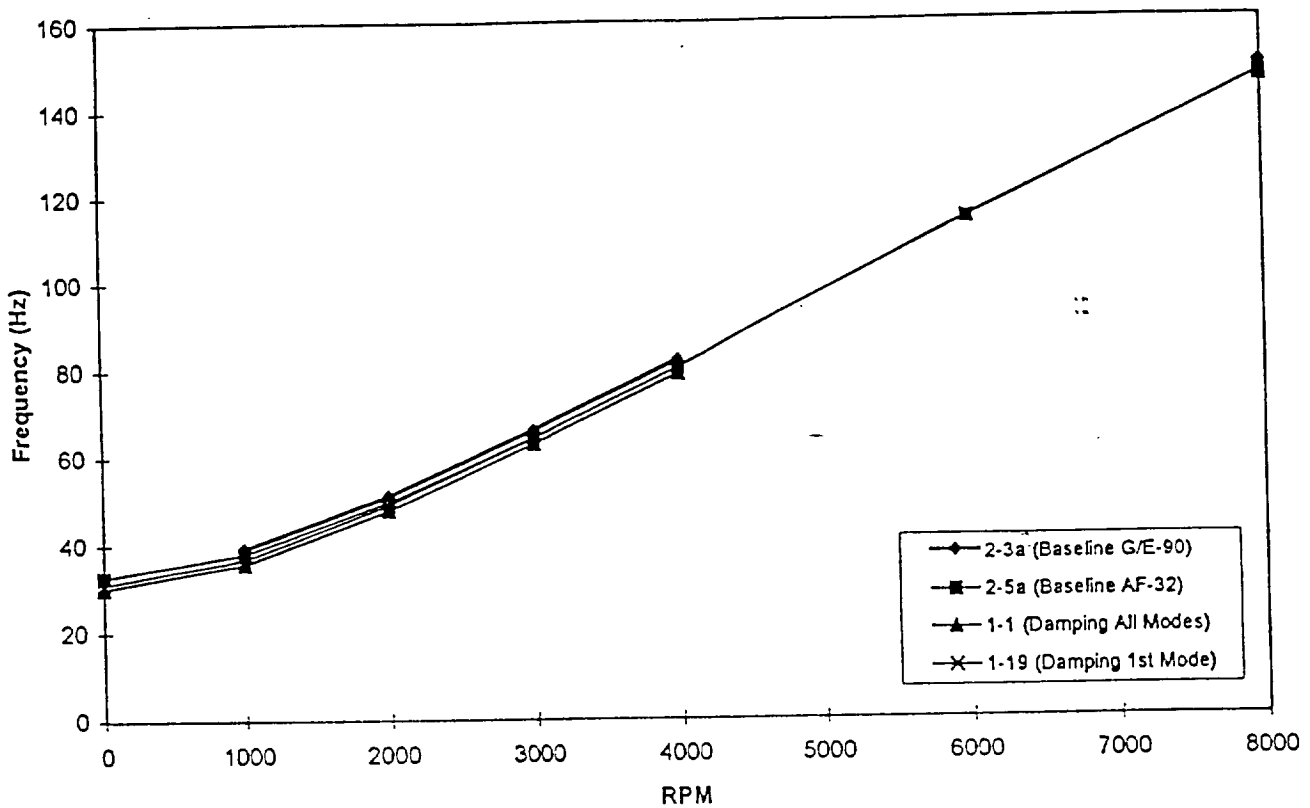


Fig. 6.b: Variation of 1st Bending Damping (1st Peak) with Rotor Speed:  
Flat Plate

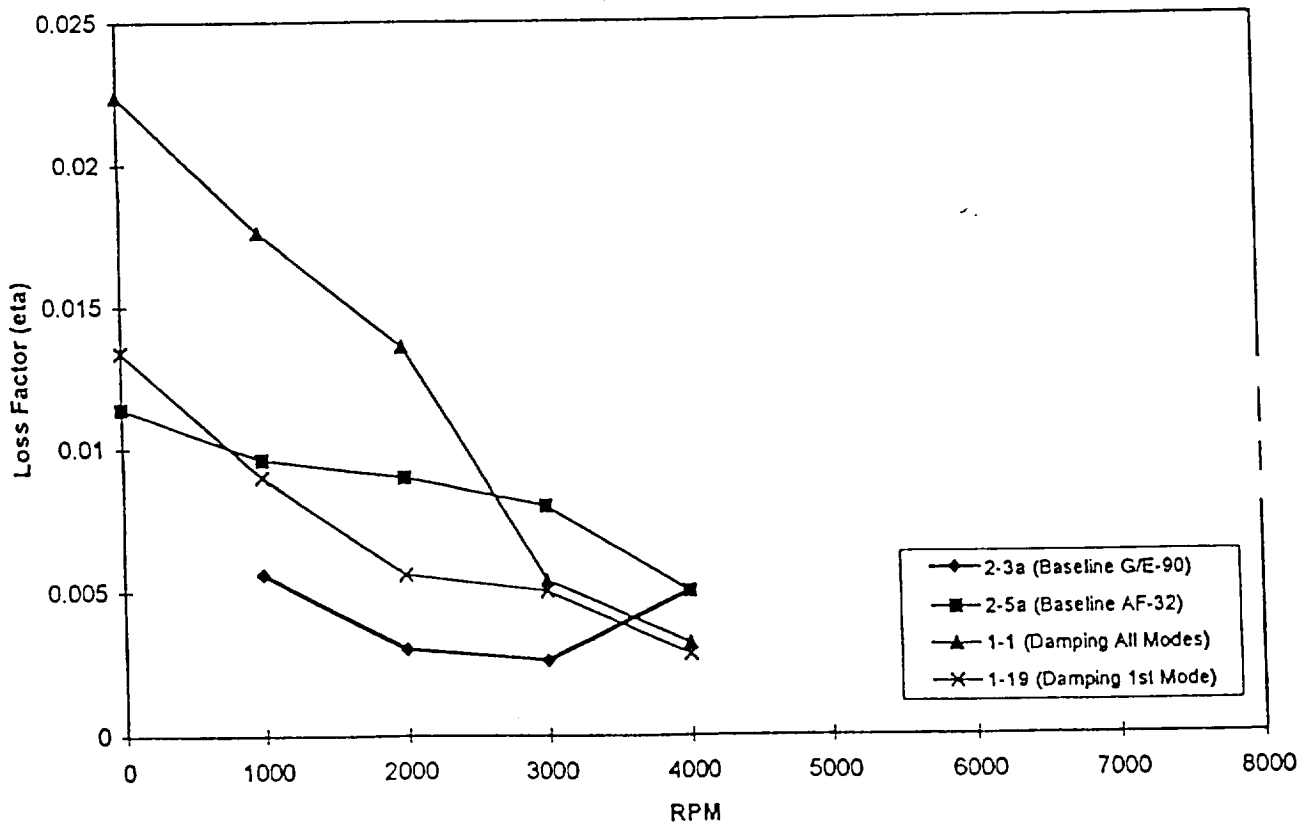


Fig. 7.a: Variation of 2nd Bending Frequency with Rotor Speed: Flat Plate

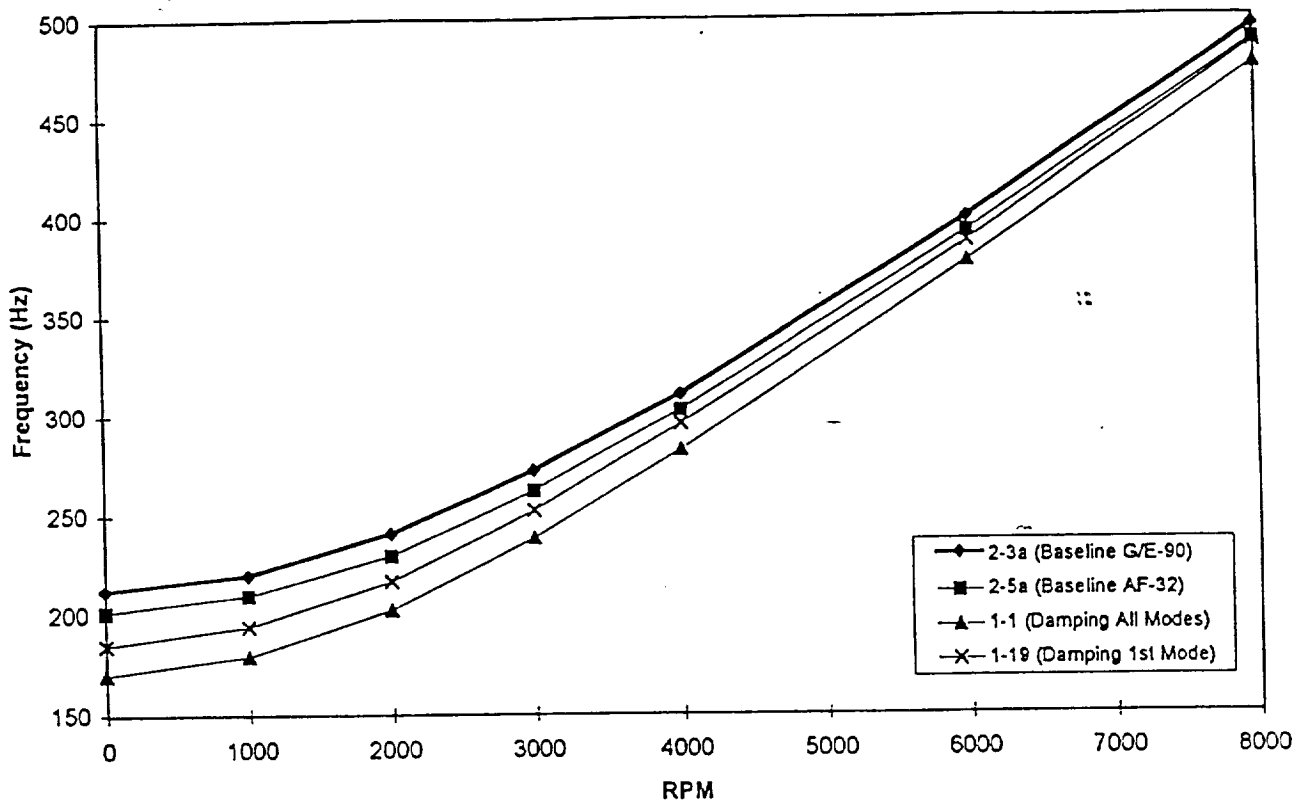


Fig. 7.b: Variation of 2nd Bending Damping with Rotor Speed: Flat Plate

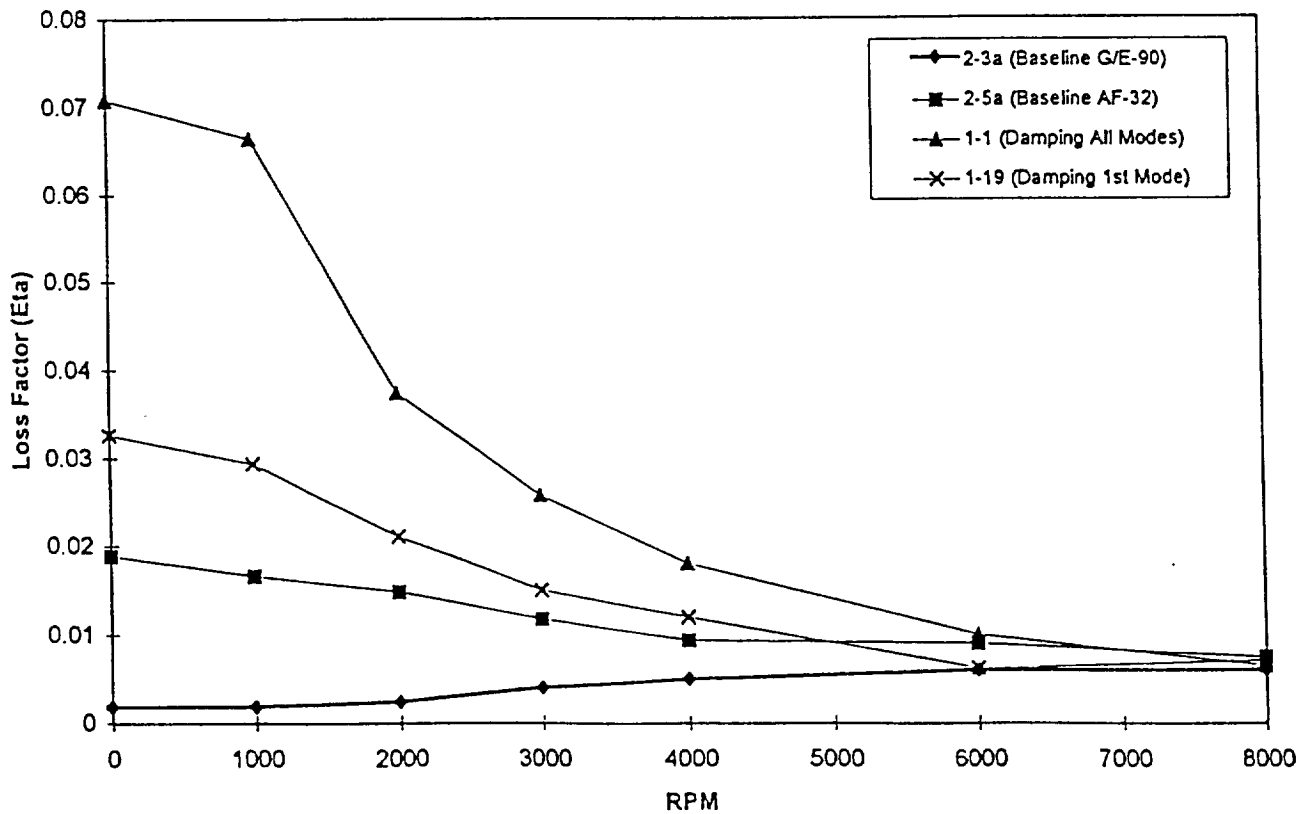


Fig. 8.a: Variation of 1st Torsion Frequency with Rotor Speed: Flat Plate

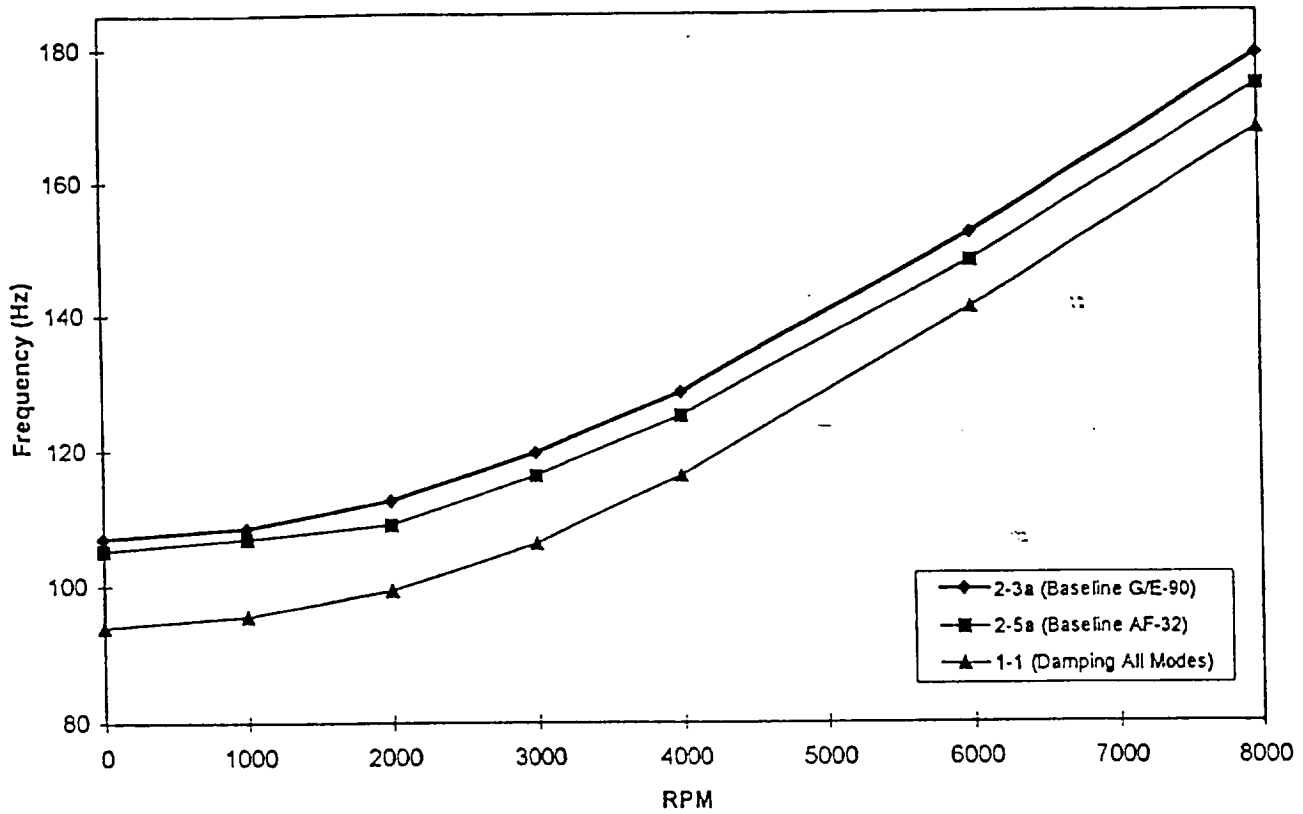
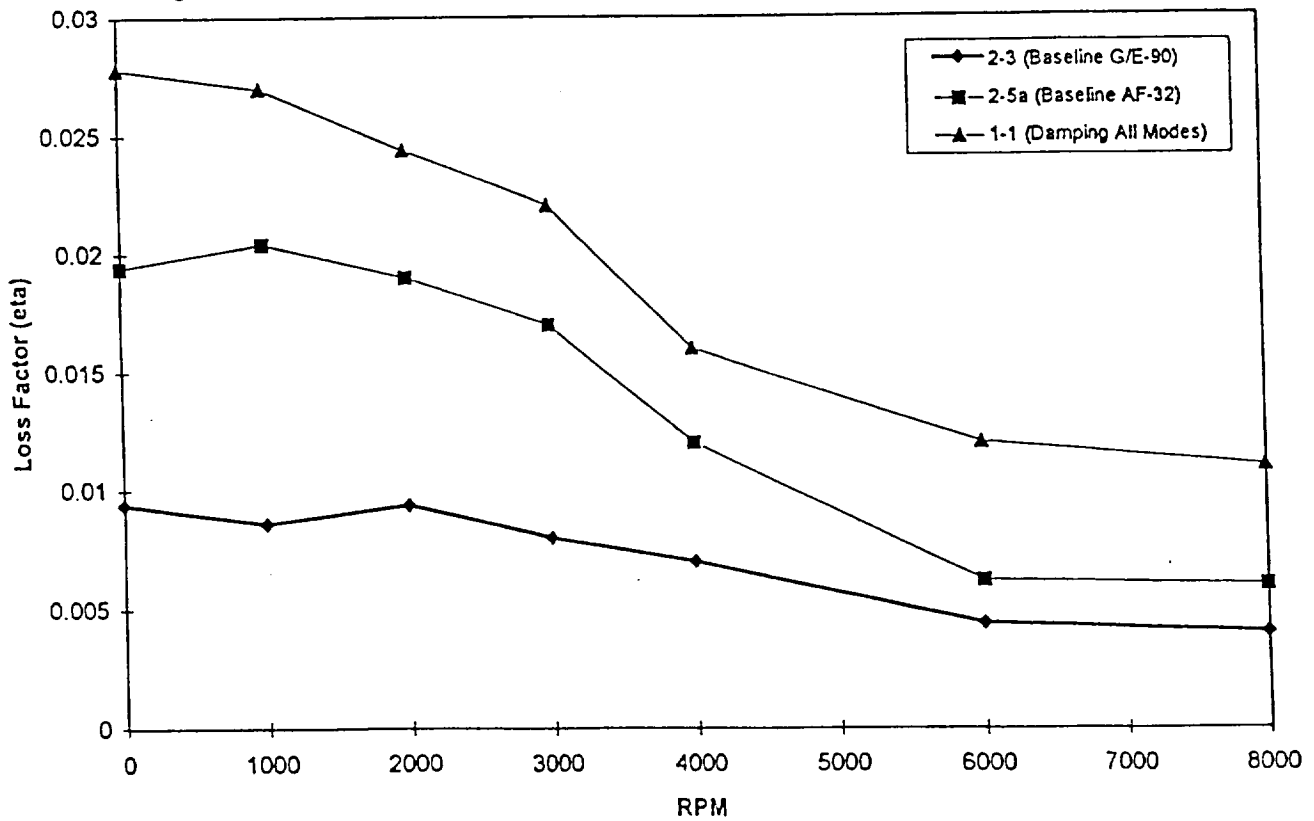


Fig. 8.b: Variation of 1st Torsion Damping with Rotor Speed: Flat Plate



the reduction of the damping levels with rotor speed. These reductions in damping levels are not due to failure of damping material, but rather a result of the centrifugal forces that stiffens the plate and lowers the strains in the damping material and thus producing less energy loss in the damping layer. Stated another way, loss factor is defined as the vibration energy dissipated divided by the vibration energy stored in the structure. As the structure stiffens the denominator increases, causing the loss factor decrease. In Figures (7.a, b) and (8.a,b), the natural frequency and damping levels of the second bending mode and the first torsion mode of the four flat plates are presented as a function of rotational speed. For these higher frequency modes, it was easy to determine the frequency and damping up to 8000 rpm. Again, these results clearly show the significant increase in bending and torsion frequencies and reduction of the damping levels with rotor speed.

The frequency and damping (loss factor) results of the spinning **pretwisted (30 degree)** plate study is presented in Figure 9-11, for the first bending, second bending, and first torsion modes respectively. The experimental results for the six plates are presented using solid lines and symbols, where the included dashed lines are analytically calculated changes in the damping level with rotational speed (i.e. centrifugal stiffening effects on damping). Both of the bending modes results (Figs. 9, 10) clearly show the increase in frequency and decrease in modal damping levels with rotational speed, where the analytical predictions closely match the trends. The variation of the first torsion frequency and damping level with rotational speed is presented in Figure 11. For this highly pretwisted plate, the centrifugal force has the tendency to untwist the plate thereby lowering its natural frequency or softening the torsion stiffness of the plate. Then, as expected, this softening of the plate causes an increase in the corresponding damping levels.

Fig. 9.a: Variation of First Bending Mode Frequency With Rotor Speed for Twisted Plates

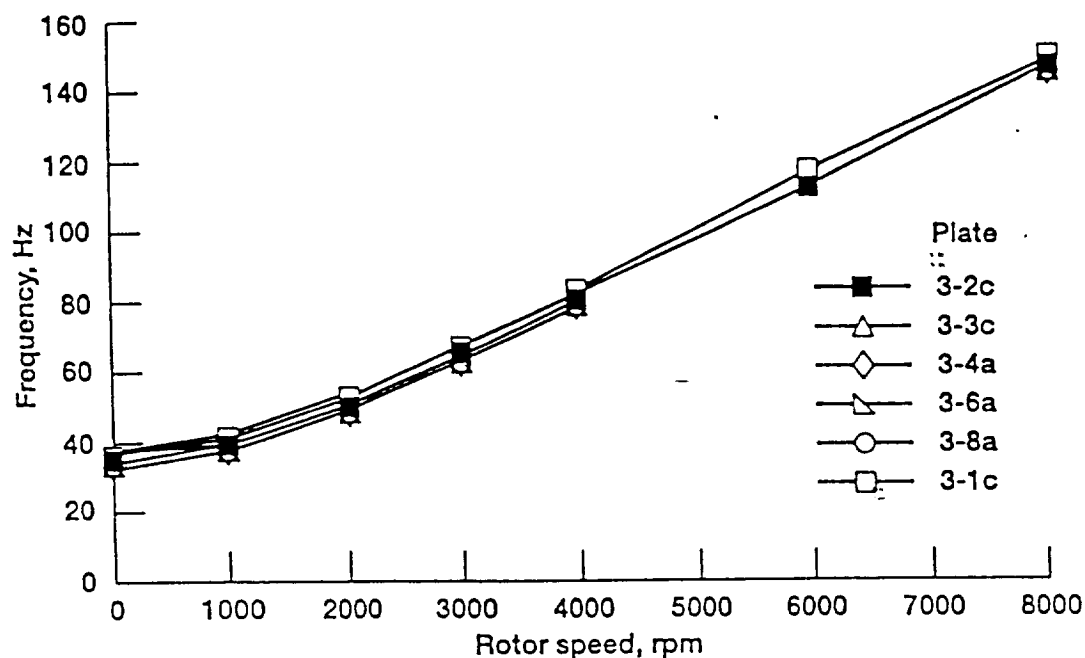


Fig. 9.b: Variation of First Bending Mode Damping With Rotor Speed for Twisted Plates

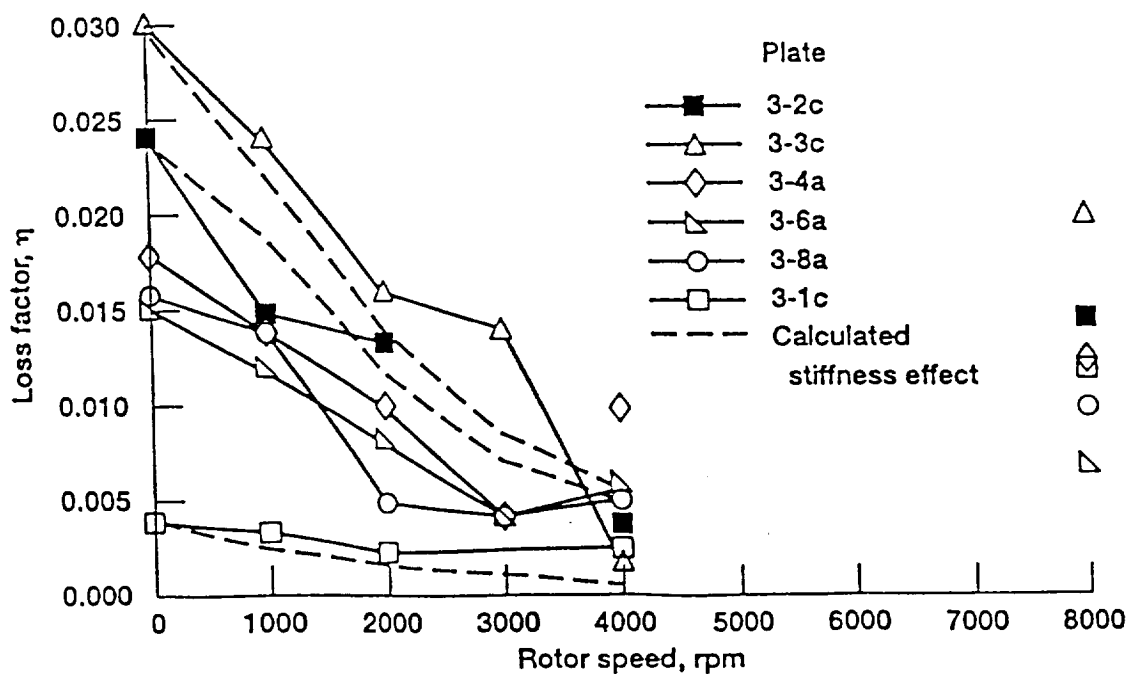


Fig. 10.a: Variation of Second Bending Mode Frequency With Rotor Speed for Twisted Plates

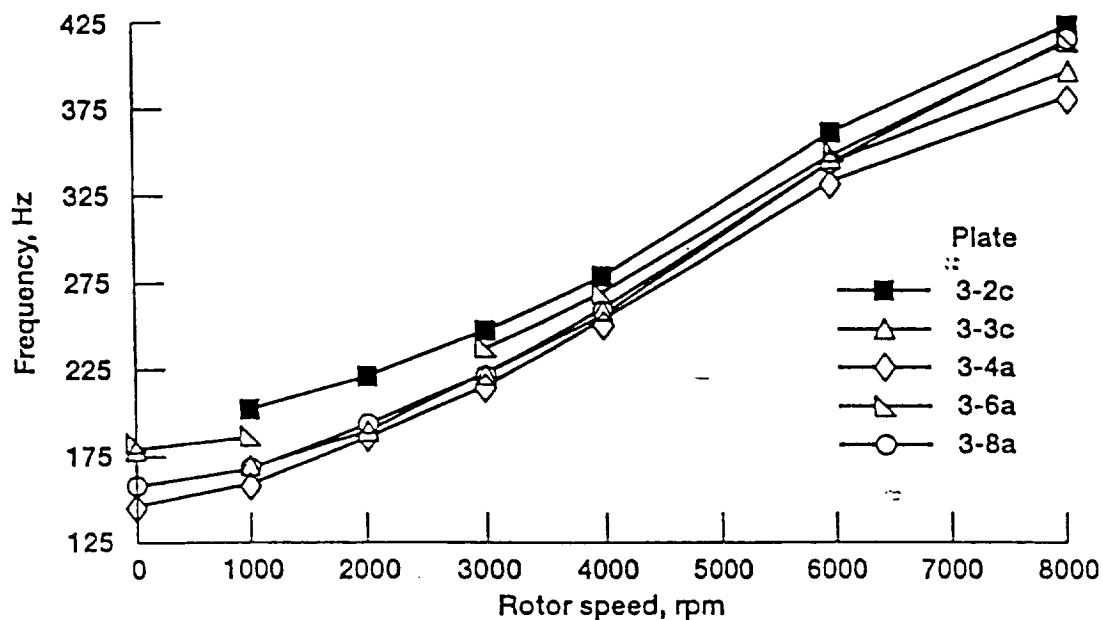


Fig. 10.b: Variation of Second Bending Mode Damping With Rotor Speed for Twisted Plates

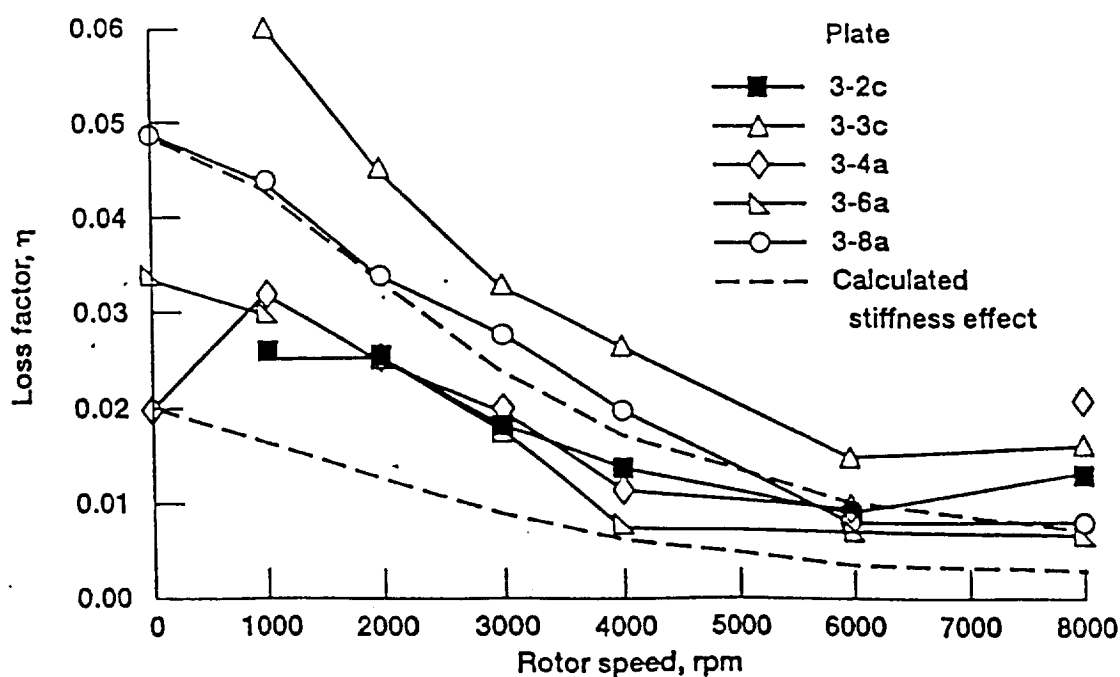


Fig. 11.a: Variation of First Torsion Mode Frequency With Rotor Speed for Twisted Plates

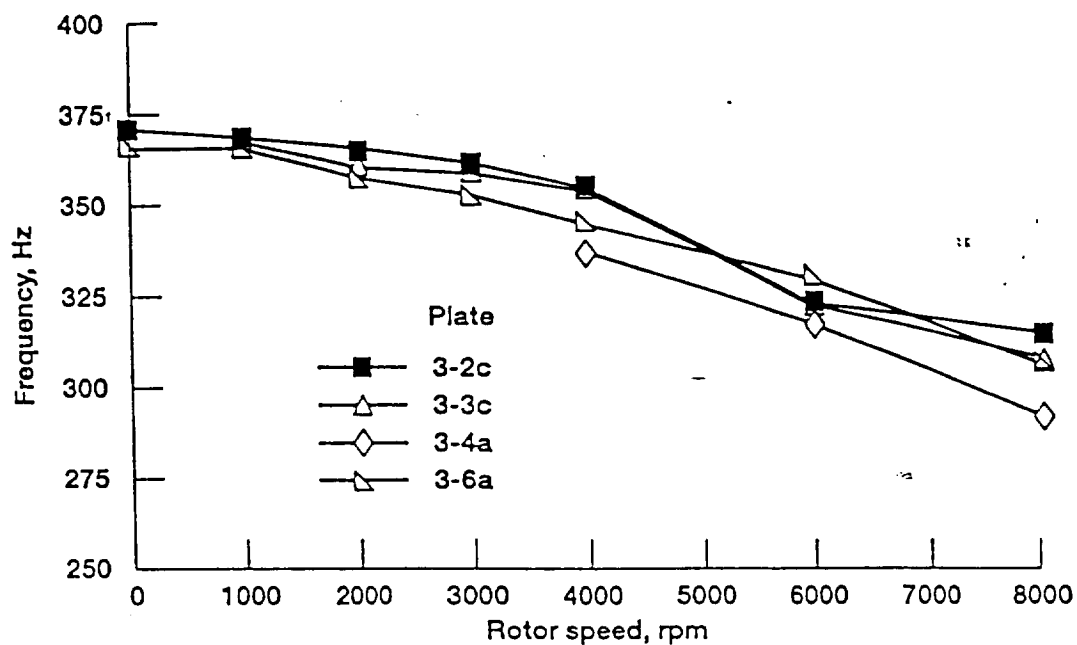
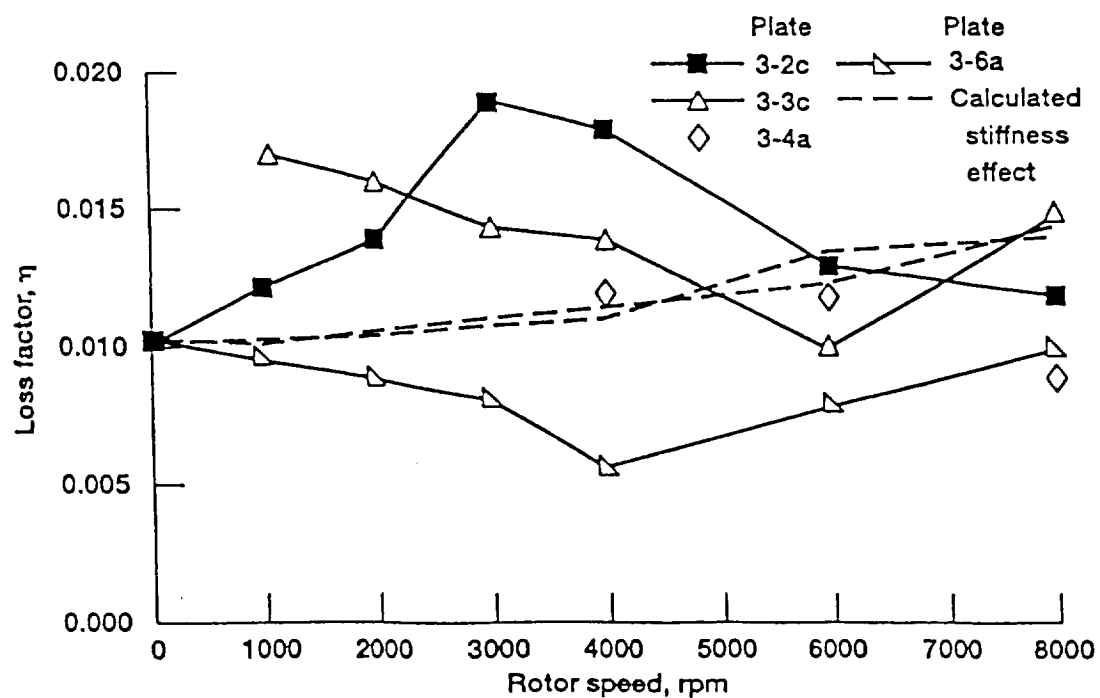


Fig. 11.b: Variation of First Torsion Mode Damping With Rotor Speed for Twisted Plates



## 5. CONCLUSIONS

Experimental data has been presented from a vibration spin experiment of flat and twisted graphite composite plates damped with 3M ISD 113 viscoelastic damping material embedded between composite layers. Damping was calculated from measured transfer functions of blade strain to blade base accelerometer data. Damping was repeatable and there was no failures or delaminations of the plates. This is significant since 3M ISD-113 has a very low creep modulus at room temperature, and the plates had up to 28,000 g's centrifugal load at the tip. Centrifugal stiffening was large for the plates and caused a significant increase in the bending natural frequencies and a corresponding decrease in the modal damping levels. However, real fan blades have smaller increases in natural frequency with rotational speed, and therefore, the decrease in fan blade damping should be smaller than measured in this experiment.

## 6. REFERENCES

1. Kosmatka, J.B., and O. Mehmed; "Passive Reduction of Advanced Composite Pretwisted Plates Using Integral Damping Materials," Proceedings of the 1995 SPIE Smart Materials and Structures Conference, vol. 2445, pp 72-83, 1995.
2. Nabi, S. M. and N. Ganesan, "Vibration and Damping Analysis of Pre-Twisted Composite Blades," Computers and Structures, vol. 47, no. 2, pp. 275-280, 1993.
3. Barrett, D. J., "On the Use of Stress Coupling in Damped Plates," Journal of Sound and Vibration, vol. 60, no. 1, pp. 187-191, 1993.
4. Sun, C. T., B. V. Sankar, and V. S. Rao, "Damping and Vibration Control of Unidirectional Composite Laminates Using Add-On Viscoelastic Materials," Journal of Sound and Vibration, vol. 139, no. 2, pp. 277-287, 1990
5. Saravanos, D.A., and J. M. Pereira, "Effect of Interply Damping Layers on the Dynamic Characteristics of Composite Plates," AIAA Journal, vol. 30, no. 12, pp. 2906-2913, 1992.
6. Kosmatka, J. B., A. J. Lapid, & O. Mehmed; "Passive Vibration Reduction of Advanced Composite Pre-Twisted Plates Using Integral Damping Materials," Proceedings of the 1995 SPIE Symposium on Smart Structures and Materials, vol. 2445, no. 8, pp. 72-83, 1995.

